RESEARCH ARTICLE

annalen der physik
www.ann-phys.org

Brownian Particle in a Poisson-Shot-Noise Active Bath: Exact Statistics, Effective Temperature, and Inference

*Costantino Di Bello, Rita Majumdar, Rahul Marathe, Ralf Metzler, and Édgar Roldán**

The dynamics of an overdamped Brownian particle in a thermal bath that contains a dilute solution of active particles is studied. The particle moves in a harmonic potential and experiences Poisson shot-noise kicks with specified amplitude distribution due to moving active particles in the bath. From the Fokker–Planck equation for the particle dynamics, the stationary solution for the displacement distribution is derived along with the moments characterizing mean, variance, skewness, and kurtosis, as well as finite-time first and second moments. An effective temperature is also computed through the fluctuation–dissipation theorem and show that equipartition theorem holds for all zero-mean kick distributions, including those leading to non-Gaussian stationary statistics. For the case of Gaussian-distributed active kicks, a re-entrant behavior from non-Gaussian to Gaussian stationary states and a heavy-tailed leptokurtic distribution across a wide range of parameters are found as seen in recent experimental studies. Further analysis reveals statistical signatures of the irreversible dynamics of the particle displacement in terms of the time asymmetry of cross-correlation functions. Fruits of the work is the development of an compact inference scheme that may allow experimentalists to extract the rate and moments of underlying shot-noise solely from the statistics the particle position.

1. Introduction

Following the probabilistic description of Brownian motion by Einstein and Smoluchowski,[1,2] Langevin introduced the concept of the fluctuating force,[3] to capture (schematically[4]) the motion of a single particle. Fluctuating forces have meanwhile become a key principle in the formulation of non-equilibrium statistical physics.[5–7] We note that the classically considered systems are connected to a thermal bath, effecting, inter alia, the temperature dependence of the diffusion coefficient of a Brownian particle embodied in the Einstein–Smoluchowski relation.[8]

The search for fundamental laws governing stochastic processes in a non-equilibrium system is one of the most active fields of research within statistical physics. While thermodynamic laws are well established in the context of equilibrium macroscopic systems,[9] their understanding turns out to be significantly more challenging when studying the erratic motion of microscopic non-equilibrium systems, such as unicellular organisms, which lead to fluctuating transfer of energy and matter. Stochastic thermodynamics is currently playing a central role in establishing a theoretical framework to study small systems far from equilibrium, in which fluctuations and randomness play a significant role.[10,11]

A key goal of contemporary non-equilibrium thermodynamics is to find universal principles governing the behavior of active matter. Active matter has recently attracted considerable attention in statistical physics, biophysics, and soft matter.[12–14] Popular toy-models in statistical physics of active matter are the so-called (microscopic) active particles, which exhibit self-propulsion in fluctuating media by consuming and dissipating internal and environmental sources of energy. Such models have been very successful in describing experimental records of the motion of, for example, bacterial suspensions of different types of bacteria or light or chemical gradient controlled artificial microswimmers.[14,15] Active systems operate away from equilibrium and thus do not satisfy classical detailed balance nor a fluctuation-dissipation relation—but follow recently discovered principles derived in the framework of stochastic thermodynamics.[16–21] It is customary to describe the motion of active particles using overdamped Langevin equations, in which an active noise component is considered along with the thermal Gaussian white noise, giving rise to non-trivial statistics.[13,14] Examples include Ornstein–Uhlenbeck noise, run-and-tumble motion, telegraphic, Lévy, and Poisson shot noise.[22–27] In general, it is not possible to derive exact analytical expressions for the emerging statistics (e.g.,

C. Di Bello, R. Metzler
Institute of Physics & Astronomy
University of Potsdam
14476 Potsdam, Germany
R. Majumdar, R. Marathe
Department of Physics
Indian Institute of Technology
Delhi, Hauz Khas, New Delhi 110016, India
R. Majumdar, É. Roldán
QLS section
ICTP – The Abdus Salam International Centre for Theoretical Physics
Trieste 34151, Italy
E-mail: edgar@ictp.it
R. Metzler
Asia Pacific Centre for Theoretical Physics
Pohang 37673, Republic of Korea

The ORCID identification number(s) for the author(s) of this article can be found under https://doi.org/10.1002/andp.202300427

DOI: 10.1002/andp.202300427

finite-time moments, stationary distribution, etc.) of Langevin equations with active noise, with the exception of few examples for which such calculations becomes a formidable task.[28–30]

A fundamental question in statistical physics is the interaction of thermal energy and confinement. At equilibrium, the particle displacement in a conservative force field is described by the Boltzmann distribution.[8,9] Of particular interest in physics is the linear Hookean force field. In a thermal bath this corresponds to the Brownian harmonic oscillator.[6] For colloidal particles a linear force can be implemented experimentally by optical tweezers.[31] While the relaxation dynamics of the colloidal particle toward equilibrium may be non-exponential in complex fluids,[32] the equilibrium distribution typically remains Gaussian in a thermal bath, with an externally tunable width depending on the force constant of the tweezers trap.

Optical tweezers setups can also be immersed in active reservoirs. Such studies showed that the displacement distribution of the confined particle becomes progressively non-Gaussian with increasing activity of the (bacterial) bath.[15,33–38] The distribution of the system exhibits a concentrated central region with heavier-than-Gaussian tails, thereby enhancing the system dynamics.[36,39–47] Under the influence of coloured noise, two approximations to the stationary probability distribution for Langevin dynamics with colored Ornstein-Uhlenbeck noise in conservative potentials are extensively investigated in literature (Fox[48] and UCNA[49]). Recently, several approximations have been introduced for stochastic systems that relax to a non-equilibrium stationary state in the presence of colored noise. In a 1D active system, the precise stationary probability distribution is evaluated rarely, for example, for run-and-tumble dynamics.[50] In a system composed of interacting active particles, the explicit formula for the non-equilibrium stationary probability distribution is achieved using the unified colored noise approximation (UCNA)[51] as well as Fox's approximation.[52] For active-Ornstein–Uhlenbeck particles (AOUPs), the steady-state distribution is calculated at a small but finite persistence time. The particle shows a non-Boltzmann distribution but still maintains detailed balance.[53]

A plausible model for the noise exerted by a dilute solution of active systems (e.g., bacteria) to an optically-trapped colloidal particle is a sequence of active kicks with arrivals at random Poissonian times. Such noise has also been used to describe recent experiments in soft[36,54] and granular matter.[29] Analytically solving the Fokker–Planck equation with such a form of non-Gaussian active noise poses a considerable challenge. Thus, in this context, we here address the Fokker–Planck equation for a linear stochastic model in the presence of both thermal (Gaussian white) and active Poisson shot noise (PSN), aiming to calculate the stationary probability density, along with closed-form solutions for its moments. PSN has recently captured the interest of the statistical physics community due to its rich and complex phenomenology.[22,29,58,61–63] One of the key results of this research line was the derivation of the Fokker–Planck equation associated with the Langevin description of stochastic models subject to PSN. In ref. [58] it was shown how PSN can be seen as the limit of a dichotomous Markov process. In particular, it was observed that PSN can significantly affect the statistical properties of a particle in a thermal bath subjected to a periodic potential, either inducing absolute negative mobility,[22] or enhancing its transport properties.[59–61] Ref. [62] discusses the non-Gaussianity of this process and shows how the microscopic rate of jumps is connected to the macroscopic stationary probability of the process. The same authors discuss in ref. [63] how to solve the model with an arbitrary non-linear frictional force. It was also shown[64] how a system with PSN can exhibit a Brownian yet non-Gaussian behavior having a mean squared displacement increasing with time while possessing a non-Gaussian distribution of the position (see also[66] for more details). It has also been found[65] that a particle in a bath with PSN can have a much more efficient escape rate with respect to the case of pure Gaussian white noise. These results were illustrated with efficient methods of simulating stochastic differential equations with PSN in [67, 68].

In this paper we consider a minimal Langevin dynamics model for an overdamped Brownian particle that is confined in a harmonic potential and immersed in diluted solution of active systems, that is, the particle is simultaneously subject to a thermal and an active noise, the latter being modeled by a PSN. The PSN here implies that in an infinitesimal time interval dt there is a probability rdt that the particle receives a shot, or kick, instantaneously shifting its position from $x(t)$ to $x(t+dt) = x(t) + \text{shot}$. Each kick is considered to be independent of the position at time t, and all kicks are independent identically distributed (i.i.d.) random variables. The intensity of the kicks may come from some specified probability density function (PDF). For simplicity, we have assumed instantaneous kicks, see, for example, ref. [70] for a generalization to PSN with finite duration pulses. The mathematical formulation of such a stochastic process was discussed in refs. [55, 56], and its steady-state distribution was obtained in ref. [57].

The rest of this work is organized as follows. In Section 2, we introduce our setup, a Langevin equation describing the motion of a trapped Brownian particle that is subject to Gaussian white and Poisson shot noises, and we establish the Fokker–Planck equation (FPE) associated with its dynamics. In Section 3 we derive exact analytical expressions for the stationary PDF and the moments of the particle position from the FPE. To this aim we solve the FPE in the rather general setting in which the amplitude of the PSN is generated from a specified distribution. Next, we link our model to a possible experimental scenario, providing an exact inference method for the PSN kick statistics. Then we derive general results related to the effective temperature for our model in terms of the Onsanger regression principle. In Section 4 we consider a specific case of the Gaussian distribution of the PSN and derive analytical results. For this example, we discuss the notion of the effective temperature and provide insights about the non-Gaussianity of the process through a detailed analysis of the excess kurtosis. We conclude in Section 5 with some remarks in relation with recent soft-matter experiments with active matter, and provide insights about irreversibility and dissipation of our model. Details of the derivations, like calculations of two non-stationary moments and long-time susceptibility, and details of numerical simulations are relegated to the appendices.

2. Model

We consider a 1D overdamped Brownian particle trapped in the harmonic potential $U(x) = \kappa x^2/2$ of force constant κ that is in

simultaneous contact with a thermal bath and an active bath. The overdamped Langevin equation describing the motion of the Brownian particle then reads

$$\gamma \dot{X}_t = -\kappa X_t + \sqrt{2k_B T\gamma}\xi_t + \gamma\eta_t \tag{1}$$

where X_t is the particle position at time t, γ is the friction coefficient, k_B is the Boltzmann constant, and T is the temperature of the thermal bath. The stochastic force ξ_t is a Gaussian white noise with zero mean $\langle\xi_t\rangle = 0$ and autocorrelation $\langle\xi_t\xi_{t'}\rangle = \delta(t-t')$. The term η_t is a stochastic force, which models instantaneous random displacements experienced by the particle as a result of a kick received from constituent particles of an active bath. We assume that these kicks occur with Poissonian waiting times with constant rate ω, that is, η_t is a PSN that can be written as[56]

$$\eta_t = \sum_{i=1}^{N_t} Y_i \delta(t - t_i) \tag{2}$$

Here, Y_i is the positional displacement experienced by the particle due to the ith active kick. Furthermore, t_i are the arrival times of a Poisson counting process with rate ω, and N_t is the total number of kicks occurring up to time t. Hence, the PDF of N_t, $P(n,t) = P(N_t = n)$, is Poissonian and given by

$$P(n,t) = \exp(-\omega t)\frac{(\omega t)^n}{n!} \tag{3}$$

As mentioned, we assume that the sequence Y_i of kick amplitudes is an i.i.d. process with dimension of length in which each Y_i is sampled from a predefined PDF $\rho_a(y)$. Under these assumptions, it follows that the process η_t has the following statistical features

$$\langle\eta_t\rangle = \omega\langle Y\rangle_a, \quad \langle\eta_t\eta_s\rangle - \langle\eta_t\rangle\langle\eta_s\rangle = \omega\langle Y^2\rangle_a\delta(t-s) \tag{4}$$

where $\langle Y^n\rangle_a$ denotes the nth moment of the PDF ρ_a. Moreover, we also assume that the two noises ξ_t and η_t are independent, that is, $\langle\xi_t\eta_s\rangle = \langle\xi_t\rangle\langle\eta_s\rangle = 0$. We finally introduce the characteristic relaxation time

$$\tau \equiv \frac{\gamma}{\kappa} \tag{5}$$

which allows us to rewrite Equation (1) in the more convenient form

$$\tau\dot{X}_t = -X_t + \sqrt{2\tau\frac{k_B T}{\kappa}}\xi_t + \tau\eta_t \tag{6}$$

We may decompose the Langevin Equation (6) into the two separate component stochastic processes $X_{1,t}$ and $X_{2,t}$ such that $X_t = X_{1,t} + X_{2,t}$, allowing us to write

$$\tau\dot{X}_{1,t} = -X_{1,t} + \sqrt{2\tau\frac{k_B T}{\kappa}}\xi_t \tag{7}$$

$$\tau\dot{X}_{2,t} = -X_{2,t} + \tau\eta_t \tag{8}$$

The initial conditions are such that $X_0 = X_{1,0} + X_{2,0}$. The formal solutions of the Langevin equations for $X_{1,t}$ and $X_{2,t}$ read

$$\begin{aligned} X_{1,t} &= \exp(-t/\tau)\left[X_{1,0} + \sqrt{\frac{2k_B T}{\tau\kappa}}\int_0^t \mathrm{d}s\xi_s\exp(s/\tau)\right] \\ X_{2,t} &= \exp(-t/\tau)\left[X_{2,0} + \int_0^t \mathrm{d}s\eta_s\exp(s/\tau)\right] \end{aligned} \tag{9}$$

Thus, after summation we get

$$X_t = \exp(-t/\tau)\left[X_0 + \int_0^t \mathrm{d}s\left(\sqrt{\frac{2k_B T}{\tau\kappa}}\xi_s + \eta_s\right)\exp(s/\tau)\right] \tag{10}$$

which is precisely the solution of Equation (1). Clearly, this factorization also holds in the stationary state. By denoting with $X = \lim_{t\to\infty} X_t$, with $X_1 = \lim_{t\to\infty} X_{1,t}$ and $X_2 = \lim_{t\to\infty} X_{2,t}$ we obtain that $X = X_1 + X_2$. Since X is the sum of two independent random variables, we can use some simple identities to compute its moments, variance, skewness and kurtosis, as we will show in Section 3.

Figure 1 sketches a possible experimental realization of our model in which a colloidal particle is embedded in a Newtonian fluid at temperature T and trapped in a static harmonic potential created, for example, by optical tweezers. The colloid is put in contact with a non-equilibrium bath of self-propelled bacteria. The bacterial activity may be tuned externally (e.g., by setting a constant concentration of nutrients) in such a way that both the kick rate ω and the amplitude distribution $\rho_a(Y)$ of the kicks exerted on the particle can be maintained at a steady level. Furthermore, the particle and bacteria may be trapped in a periodic chamber where fluid flows at a constant speed giving rise to an asymmetric bacterial kick distribution $\langle Y\rangle_a \neq 0$ (Figure 1, left panel), or in a closed chamber for which the bacterial kick distribution is symmetric around zero $\langle Y\rangle_a = 0$ (Figure 1, middle panel).

The colloid dynamics shows some exciting behavior as we change the mean spiking rate ω or the bacterial activity. Here, we present some trajectories of the particle driven by the active noise (Equation (56) and Section 4) for different ω. It is evident that for small ω the average value of the position of the colloid is close to zero, and it behaves like a Gaussian process. As we increase the rate ω, the jumps in the trajectory become prominent, and the system is far from equilibrium. We also varied the mean velocity of the bacteria. The green trajectory corresponds to $\mu = 0$, when a particle is optically trapped in a closed container filled with bacteria. Similarly, the red trajectory stands for the average velocity $\mu = -1$, and the blue trajectory is for $\mu = 2$, representing an optically-trapped particle in a bath with bacteria that experience a homogeneous fluid flow.

It was shown previously[55] that the above system can be described by the Fokker-Planck equation

$$\begin{aligned} \tau\frac{\partial}{\partial t}P(x,t) = \frac{\partial}{\partial x}\left[xP(x,t)\right] + \frac{k_B T}{\kappa}\frac{\partial^2}{\partial x^2}P(x,t) \\ + \omega\tau\int_{-\infty}^{\infty}[P(x-y,t) - P(x,t)]\rho_a(y)\mathrm{d}y, \end{aligned} \tag{11}$$

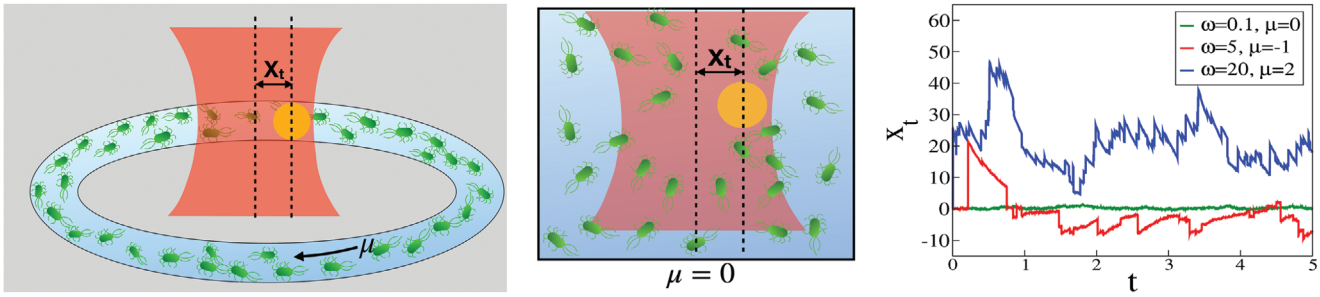

Figure 1. (Left panel) Sketch of a Brownian particle trapped with an optical tweezer within periodic boundary conditions in a dilute solution of active particles with a nonzero net average drift ($\mu \neq 0$). (Center panel) The trapped Brownian particle is subject to closed boundary conditions and immersed in a dilute active bath composed of active particles with zero net drift ($\mu = 0$). (Right panel) Representative stochastic trajectories of the Brownian particle in the active bath exerting a Poisson shot noise (PSN) on the particle (on top of the thermal noise). In this illustration, the amplitude of the kicks of the PSN is drawn from a Gaussian distribution given by Equation (56). Different colors represent trajectories for different parameter values varying the rate ω and mean value of the amplitude μ of the PSN kicks (see legend).

where $P(x,t) = \text{Prob}\{x \leq X_t < x + \mathrm{d}x\}$ denotes the probability density over space at time t, with some initial condition $P(x,0) = P_0(x)$ and with vanishing probability at the extremities, $\lim_{x\to\pm\infty} P(x,t) = 0$. We will not focus on the time-dependent probability $P(x,t)$ but rather its stationary distribution $P(x) \equiv \lim_{t\to\infty} P(x,t)$. We will use Equation (11) to derive $P(x)$. We will proceed by deriving the analytical expression for $P(x)$ with its first and second moments, skewness, and kurtosis, for arbitrary kick intensity distribution $\rho_a(y)$. We will then consider the specific case of Gaussian kick intensities, and conclude with some results concerning other intensity distributions and with some future directions of research.

3. Main Results

We now derive the stationary PDF $P(x)$. To this end, rewrite the FPE Equation (11) in the form

$$0 = \frac{\partial}{\partial x}\left[xP(x)\right] + \frac{k_B T}{\kappa}\frac{\partial^2}{\partial x^2}P(x) - \omega\tau P(x) + \omega\tau\int_{-\infty}^{\infty} P(x-y)\rho_a(y)\mathrm{d}y \tag{12}$$

where we set the left hand side to zero and used the normalization condition of ρ_a. We notice that the integral term in this integro-differential equation is just a convolution of two functions, and it is then convenient to apply a Fourier transform. We denote the respective Fourier transform of $P(x)$ and $\rho_a(y)$ by $\hat{P}(q) = \int_{-\infty}^{\infty}\exp(\mathrm{i}qx)P(x)\mathrm{d}x$ and $\hat{\rho}_a(q) = \int_{-\infty}^{\infty}\exp(\mathrm{i}qy)\rho_a(y)\mathrm{d}y$, where i is the imaginary unit. We then obtain

$$0 = -q\frac{\partial}{\partial q}(\hat{P}(q)) - \frac{k_B T}{\kappa}q^2\hat{P}(q) + \omega\tau\hat{P}(q)\hat{\rho}_a(q) - \omega\tau\hat{P}(q) \tag{13}$$

which is an ordinary differential equation with the boundary condition $\hat{P}(0) = 1$. After some simple algebra we obtain

$$q\frac{\partial\hat{P}(q)}{\partial q} = \left(-\frac{k_B T}{\kappa}q^2 + \omega\tau\hat{\rho}_a(q) - \omega\tau\right)\hat{P}(q) \tag{14}$$

from which, in turn, we find

$$\frac{\partial\ln(\hat{P}(q))}{\partial q} = -\frac{k_B T}{\kappa}q + \omega\tau\left(\frac{\hat{\rho}_a(q)-1}{q}\right) \tag{15}$$

Hence the stationary PDF in Fourier domain reads

$$\hat{P}(q) = \exp\left(-\frac{k_B T}{2\kappa}q^2\right)\exp\left(\omega\tau\int_0^q\frac{\hat{\rho}_a(q')-1}{q'}\mathrm{d}q'\right) \tag{16}$$

As we can see the previous expression is the product of the two terms

$$\hat{P}_1(q) = \exp\left(-\frac{k_B T}{2\kappa}q^2\right), \quad \hat{P}_2(q) = \exp\left(\omega\tau\int_0^q\frac{\hat{\rho}_a(q')-1}{q'}\mathrm{d}q'\right) \tag{17}$$

where $\hat{P}_1(q)$ is the characteristic function of the random variable X_1, while $\hat{P}_2(q)$ is the characteristic function of X_2. Therefore, as stated before, this confirms that $X = X_1 + X_2$, since the characteristic function of the sum of two random variables is the product of the two characteristic functions. Finally, by inverting the Fourier transform, $P(x)$ reads

$$P(x) = \int_{-\infty}^{\infty}\frac{\mathrm{d}q}{2\pi}\exp(-\mathrm{i}qx)\exp\left(-\frac{k_B T}{2\kappa}q^2 + \omega\tau I(q)\right) \tag{18}$$

where

$$I(q) \equiv \int_0^q\frac{\hat{\rho}_a(q')-1}{q'}\mathrm{d}q' \tag{19}$$

Equation (16) was already derived in ref. [57] through an alternative mathematical approach. For a given choice for ρ_a Equation (18) can be numerically implemented using the GNU Scientific Library (GSL), see Appendix D for further details. In the next subsection we will discuss the moments of the random variables X, X_1, and X_2.

3.1. Moments of the Distribution

We now derive the analytical expressions for the lower-order moments of X in the stationary state. We use the notation

$$\langle X^n \rangle = \int_{-\infty}^{\infty} x^n P(x) \mathrm{d}x \tag{20}$$

for the nth moment of the random variable X. In what follows, we will mainly focus on the variance $\mathrm{Var}[X]$, skewness $\tilde{\mu}_3[X]$, and excess kurtosis $\mathcal{K}_{\mathrm{ex}}[X]$ of the random variable X. The general expressions for these central statistical quantities, in terms of the central moments of X, are given by

$$\mathrm{Var}[X] \equiv \langle (X - \langle X \rangle)^2 \rangle, \quad \tilde{\mu}_3[X] \equiv \frac{\langle (X - \langle X \rangle)^3 \rangle}{\mathrm{Var}[X]^{3/2}},$$
$$\mathcal{K}_{\mathrm{ex}}[X] \equiv \frac{\langle (X - \langle X \rangle)^4 \rangle}{\mathrm{Var}[X]^2} - 3 \tag{21}$$

The statistical quantities defined in Equation (21) may be directly evaluated by expanding the binomials and using the identity

$$\langle X^n \rangle = \frac{1}{\mathrm{i}^n} \frac{d^n}{dq^n} \hat{P}(q) \Big|_{q=0} \tag{22}$$

where $\hat{P}(q)$ is given by Equation (16). After some algebra, we obtain the first four moments of the particle position in the stationary state

$$\langle X \rangle = \omega\tau \langle Y \rangle_a \tag{23}$$
$$\langle X^2 \rangle = \frac{k_B T}{\kappa} + \frac{\omega\tau}{2} \langle Y^2 \rangle_a + \omega^2 \tau^2 \langle Y \rangle_a^2 \tag{24}$$
$$\langle X^3 \rangle = \frac{\omega\tau}{3} \langle Y^3 \rangle_a + \omega^3 \tau^3 \langle Y \rangle_a^3 + 3\omega\tau \langle Y \rangle_a \left(\frac{k_B T}{\kappa} + \frac{\omega\tau}{2} \langle Y^2 \rangle_a \right), \tag{25}$$
$$\langle X^4 \rangle = \frac{\omega\tau}{4} \langle Y^4 \rangle_a + \frac{4\omega^2\tau^2}{3} \langle Y \rangle_a \langle Y^3 \rangle_a + \omega^4 \tau^4 \langle Y \rangle_a^4 + 6\omega^2 \tau^2 \langle Y \rangle_a^2 \left(\frac{k_B T}{\kappa} + \frac{\omega\tau}{2} \langle Y^2 \rangle_a \right) + 3 \left(\frac{k_B T}{\kappa} + \frac{\omega\tau}{2} \langle Y^2 \rangle_a \right)^2 \tag{26}$$

Substituting expressions (23)–(26) into Equation (21) we directly find the analytical expressions for the stationary variance, skewness, and excess kurtosis associated with the particle position.

We mention an alternative yet insightful way to evaluate the moments of X through the statistics of X. As mentioned, in the stationary state $X = X_1 + X_2$, with X_1 and X_2 being independent random variables. This property implies the compact expressions of the moments

$$\langle X^n \rangle = \sum_{m=0}^{n} \binom{n}{m} \langle X_1^m \rangle \langle X_2^{n-m} \rangle \tag{27}$$

and for the variance, skewness, and excess kurtosis of X in terms of those of X_1 and X_2[69]

$$\mathrm{Var}[X] = \mathrm{Var}[X_1] + \mathrm{Var}[X_2] \tag{28}$$
$$\tilde{\mu}_3[X] = \left(\frac{\mathrm{Var}[X_1]}{\mathrm{Var}[X_1] + \mathrm{Var}[X_2]} \right)^{3/2} \tilde{\mu}_3[X_1] + \left(\frac{\mathrm{Var}[X_2]}{\mathrm{Var}[X_1] + \mathrm{Var}[X_2]} \right)^{3/2} \tilde{\mu}_3[X_2] \tag{29}$$
$$\mathcal{K}_{\mathrm{ex}}[X] = \left(\frac{\mathrm{Var}[X_1]}{\mathrm{Var}[X_1] + \mathrm{Var}[X_2]} \right)^{2} \mathcal{K}_{\mathrm{ex}}[X_1] + \left(\frac{\mathrm{Var}[X_2]}{\mathrm{Var}[X_1] + \mathrm{Var}[X_2]} \right)^{2} \mathcal{K}_{\mathrm{ex}}[X_2] \tag{30}$$

We proceed by first discussing the moments of X_1 and of X_2, and then we will use these moments to extract closed-form expressions for the central moments of X.

3.1.1. Moments of X_1 and X_2

From Equation (17) it is clear that X_1 is a Gaussian random variable with zero mean. Hence, its first two moments are given by

$$\langle X_1 \rangle = 0, \quad \langle X_1^2 \rangle = \frac{k_B T}{\kappa} \tag{31}$$

while its skewness and excess kurtosis are equal to zero, $\tilde{\mu}_3[X_1] = \mathcal{K}_{\mathrm{ex}}[X_1] = 0$.

For X_2, instead, the central moments can be found via the identity

$$\langle (X_2 - \langle X_2 \rangle)^n \rangle = \frac{1}{\mathrm{i}^n} \frac{d^n}{dq^n} \left(\exp(-\mathrm{i}q\langle X_2 \rangle) \hat{P}_2(q) \right) |_{q=0} = \frac{1}{\mathrm{i}^n} \frac{d^n}{dq^n} \left[\exp\left(\omega\tau \left(I(q) - qI'(0) \right) \right) \right] |_{q=0} \tag{32}$$

where in the last expression we used that $\exp(-\mathrm{i}q\langle X_2 \rangle) = \exp(-(\omega\tau)qI'(0))$. It is shown in Appendix A.2 that

$$\langle X_2 \rangle = \omega\tau \langle Y \rangle_a \tag{33}$$

and that, for $n = 2, 3$

$$\langle (X_2 - \langle X_2 \rangle)^n \rangle = \frac{\omega\tau}{n} \langle Y^n \rangle_a, \tag{34}$$

while for $n = 4$

$$\langle (X_2 - \langle X_2 \rangle)^4 \rangle = \frac{1}{4} \omega\tau \langle Y^4 \rangle_a + \frac{3}{4} \omega^2 \tau^2 \langle Y^2 \rangle_a^2 \tag{35}$$

From the last two equations we can immediately get the variance, the skewness, and the kurtosis of X_2

$$\mathrm{Var}[X_2] = \frac{1}{2} \omega\tau \langle Y^2 \rangle_a, \quad \tilde{\mu}_3[X_2] = \sqrt{\frac{8}{9\omega\tau}} \frac{\langle Y^3 \rangle_a}{\sqrt{\langle Y^2 \rangle_a^3}},$$
$$\mathcal{K}_{\mathrm{ex}}[X_2] = \frac{1}{\omega\tau} \frac{\langle Y^4 \rangle_a}{\langle Y^2 \rangle_a^2} \tag{36}$$

3.1.2. Mean, Variance, Skewness, and Excess Kurtosis of X

We can now obtain the mean, the variance, the skewness, and the excess kurtosis of X from expressions (27)–(30), and the results of Section 3.1.1. Thus

$$\langle X\rangle = \omega\tau\langle Y\rangle_a \tag{37}$$

that is, the average of the position is directly proportional to the average of ρ_a and to the rate of kicks ω. The variance reads

$$\mathrm{Var}[X] = \frac{k_B T}{\kappa} + \frac{\omega\tau}{2}\langle Y^2\rangle_a \tag{38}$$

Hence, as expected from Equation (28), on the right hand side a thermal and an active contribution appear. Interestingly, the active contribution, which is basically the variance of X_2, scales as $\omega\tau$, just as the mean. This linear dependence on $\omega\tau$ is an effect of the central limit theorem: both the mean and the variance must scale as the mean number of events in a characteristic time—which is indeed $\omega\tau$.

The skewness of the process X reads

$$\tilde{\mu}_3[X] = \sqrt{\frac{8}{9}\omega\tau}\left(\frac{2k_B T}{k} + \omega\tau\langle Y^2\rangle_a\right)^{-3/2}\langle Y^3\rangle_a \tag{39}$$

Interestingly, the distribution of X is skewed if and only if X_2 is. Note that having an amplitude distribution of kicks with zero skewness does not imply that X_2 is not skewed as well. Finally, the excess kurtosis yields in the form

$$\mathcal{K}_{\mathrm{ex}}[X] = \omega\tau\langle Y^4\rangle_a\left(\frac{2k_B T}{\kappa} + \omega\tau\langle Y^2\rangle_a\right)^{-2} \tag{40}$$

which only depends on positive quantities, thus the distribution is always leptokurtic. This result is in line with experimental observations for colloidal particles immersed in bacterial and engineered reservoirs.[15,36] Moreover, when considering T, κ, and the distribution $\rho_a(\gamma)$ as fixed, we can find an optimal value of ω maximizing the excess kurtosis

$$\omega^* = \frac{2k_B T}{\kappa\tau\langle Y^2\rangle_a} \tag{41}$$

returning the value $\mathcal{K}^\star_{\mathrm{ex}}[X] \equiv \mathcal{K}_{\mathrm{ex}}[X]|_{\omega=\omega^*}$

$$\mathcal{K}^*_{\mathrm{ex}}[X] = \frac{\kappa\langle Y^4\rangle_a}{8k_B T\langle Y^2\rangle_a} \tag{42}$$

In the limit when $\omega \ll \tau$, when the kicks are rare, both the skewness and the excess kurtosis vanish, and we retrieve the results of a Brownian particle in a quadratic potential.

3.2. Inferring the Statistics of the Underlying Active Kicks

Let us now establish a link with realistic experimental scenarios. Both the rate ω and the distribution $\rho_a(\gamma)$, characterizing the PSN, are in general not directly measurable from experiments. On the other hand, the positions of the particles are directly measurable so it in general possible to have access to the distribution $P(x)$ and its stationary moments. An interesting connection between the microscopic quantities ω and $\rho_a(\gamma)$ and the distribution $P(x)$ was obtained by Kanazawa et al. in ref. [62], where the rate ω was related to the statistics of X from the relation

$$\omega = -\lim_{q\to\infty}\left[q\frac{\partial\hat{P}(q)}{\partial q} + \frac{2k_B T}{\kappa}q^2\right] \tag{43}$$

From the results derived in Section 3.1.2 we add to the results of ref. [62] the following relations which allow us to retrieve the moments of Y from the moments of X

$$\langle Y\rangle_a = \frac{1}{\omega\tau}\langle X\rangle \tag{44}$$

$$\langle Y^2\rangle_a = \frac{2}{\omega\tau}\mathrm{Var}[X] - \frac{2k_B T}{\kappa\omega\tau} \tag{45}$$

$$\langle Y^3\rangle_a = \frac{3}{\omega\tau}\tilde{\mu}_3[X]\mathrm{Var}[X]^{3/2} \tag{46}$$

$$\langle Y^4\rangle_a = \frac{4}{\omega\tau}\mathcal{K}_{\mathrm{ex}}[X]\mathrm{Var}[X]^2 \tag{47}$$

Notably, Equations (43)–(47) provide a useful recipe for experimentalists to extract stationary statistics of the hidden stochastic process Y_t which is generally not possible under the assumption of more complex dynamics.

3.3. Effective Temperature

For a system described by an overdamped Langevin equation with active noise, one is often interested in defining an effective temperature T_{eff}.[16–18] In close-to-equilibrium passive isothermal systems an effective temperature can be defined by using either the equipartition or fluctuation–response theorems. In active systems however, mapping the non-equilibrium dynamics to an effective equilibrium dynamics is fully reliable whenever the stationary (or quasistatic) distribution is Gaussian.[73–75]

For non-Gaussian active dynamics, a possible definition of effective temperature is provided in terms the Onsanger regression principle.[76,77] We will briefly expose it here, but for a more detailed discussion we refer to refs. [17, 18, 78]. Let us consider that our system, described by Equation (1), is at stationarity. Any observable A_t has an average, that we denote with $\langle A_t\rangle$, and a correlation function defined as

$$C_A(t,s) = \langle A_t A_s\rangle \tag{48}$$

Since the system is at stationarity, the average of any observable does not depend on time, we can actually drop the dependence on t and write $\langle A_t\rangle = \langle A\rangle$. At time $t = 0$ we apply on the system a constant small force δf that modifies the Langevin equation as follows

$$\tau\dot{X}_t = -X_t + \sqrt{2\tau\frac{k_B T}{\kappa}}\xi_t + \tau\eta_t + \frac{\delta f}{\kappa} \tag{49}$$

During the relaxation toward a new steady state, any observable A has a time-dependent average $\langle A_t\rangle_f$ depending on the force δf. Onsanger regression principle states that the relaxation of the

perturbed system toward the new steady state can be seen as a spontaneous equilibrium fluctuation. This translates into a simple equation[78] connecting the correlation function $C_A(t,s)$ and the time-dependent response function (also known as susceptibility) $\chi_A(t)$ here defined as

$$\chi_A(t) = \lim_{\delta f \to 0} \frac{\langle A_t \rangle_f - \langle A \rangle}{\delta f} \tag{50}$$

The Onsager relation for isothermal equilibrium systems at temperature T reads

$$\chi_A(t) = \frac{\left[C_A(t,t) - C_A(t,0)\right]}{k_B T} \tag{51}$$

Motivated by Onsager's relation we can introduce an effective temperature by the relation

$$\frac{1}{k_B T_{\text{eff}}} = \frac{\chi_A(t)}{C_A(t,t) - C_A(t,0)} \tag{52}$$

When the time t is large compared to the typical relaxation time of the system, in other words in the stationary limit $t \to \infty$, A_t and A_0 become uncorrelated, that is, $\langle A_t A_0 \rangle = \langle A \rangle^2$, thus we can rewrite Equation (52) as

$$\frac{1}{k_B T_{\text{eff}}} = \frac{1}{\text{Var}[A]} \lim_{\delta f \to 0} \frac{\langle A \rangle_f - \langle A \rangle}{\delta f} \tag{53}$$

Specializing Equation (52) to the position $A = X$ reads

$$\frac{1}{k_B T_{\text{eff}}} = \frac{1}{\text{Var}[X]} \lim_{\delta f \to 0} \frac{\langle X \rangle_{\delta f} - \langle X \rangle_0}{\delta f} = \frac{1}{\text{Var}[X]} \lim_{t \to \infty} \chi_X(t) \tag{54}$$

It is shown in appendix that the long-time susceptibility of the position reads $\lim_{t\to\infty} \chi_X(t) = 1/\kappa$. Using this result together with the exact expression for the variance [Equation (38)], we get

$$T_{\text{eff}} = \frac{\kappa}{k_B} \text{Var}[X] = T + \frac{\kappa \omega \tau}{2 k_B} \langle Y^2 \rangle_a \tag{55}$$

In general the result of T_{eff} provided by the fluctuation-dissipation theory (FDT), is different from the one obtained from the equipartition theorem. Nevertheless, in the specific case in which PSN has zero mean, that is, when $\langle Y \rangle_a = 0$, according to Equation (23) also $\langle X \rangle = 0$, and so we have that $\text{Var}[X] = \langle X^2 \rangle$. Thus in this situation, the equipartition theorem leads to the same effective temperature than the FDT. Therefore, the effective temperature could be a useful tool to map the second moment within the PSN into the second moment of an effective isothermal nonequilibrium (yet non-Gaussian) system. We remark the presence of fat (leptokurtic) tails as a footprint of the nonequilibrium dynamics, as $P(X) \neq \exp(-V(x)/k_B T_{\text{eff}})$ is not Boltzmannian. Even though the variance can be captured by an effective Gaussian model at temperature T_{eff}, it remains mandatory to employ a non-Gaussian description to capture higher-order moments such as skewness and kurtosis.[71,72] Below we now consider a particular case where kick amplitudes are drawn from the Gaussian distribution, as an application of this general discussion.

4. Gaussian Kicks

For illustrative purposes we now consider a particular form for the amplitude distribution $\rho_a(\gamma)$ of the active kicks amplitude, namely, the shifted Gaussian distribution

$$\rho_a(\gamma) = \frac{1}{Z} \exp\left(-\frac{\beta_a \gamma^2}{2 m_a} \left[\gamma - \frac{\mu}{\gamma} \right]^2 \right) \tag{56}$$

This distribution (56) is analogous to the equilibrium distribution of a free particle of mass m_a with average momentum μ and immersed in a thermal bath with temperature

$$T_a = \frac{1}{k_B \beta_a} \tag{57}$$

Here T_a is an effective temperature as it has the dimensions of temperature but it is a parameter that is not constrained by any fluctuation-dissipation relations enforcing a specific relation with the friction coefficient γ of the particle. Similarly, m_a can be understood as an effective mass of the components of the active bath that kick the Brownian particle. Furthermore, the quantity $Z = \sqrt{2\pi m_a/\beta_a \gamma^2}$ in Equation (56) is a normalization factor enforcing normalization, $\int_{-\infty}^{\infty} \rho_a(\gamma) d\gamma = 1$, and can thus be viewed as an effective partition. For analytical ease it is useful to introduce the quantities

$$\tau_a \equiv \frac{m_a}{\gamma}, \quad \lambda \equiv \frac{\mu}{\gamma} \tag{58}$$

Here, τ_a is an effective momentum relaxation time scale, and λ is a length scale given by the mean value of the Gaussian kick amplitude distribution.

We now use the expressions derived in Section 3.1 to inspect the stationary moments of the particle. Specializing Equations (37) and (38) for the Gaussian PDF (56) we find that the mean and the variance of the position in this case become

$$\langle X \rangle = \omega \tau \lambda, \quad \text{Var}[X] = \frac{k_B T}{\kappa} + \frac{\omega \tau}{2} \left(k_B T_a \frac{\tau_a}{\gamma} + \lambda^2 \right) \tag{59}$$

These formulas have a simple interpretation: the average position is proportional to the average amplitude μ of the kicks and to their occurrence rate. At the same time, it is inversely proportional to the stiffness of the potential: the stiffer the potential is the more the particle is forced to stay close to the origin. The variance of the position is given by the sum of two contributions: $k_B T/\kappa$ associated with the thermal bath, and the contribution due to the active kicks. The contribution of the second term can be manipulated externally by changing the bacterial activity, for example, by tuning the rate ω of active kicks, the mean amplitude μ, and variance, which can be controlled via m_a and/or T_a. In practice, a bacterial suspension will be associated with given values of β_a and m_a, that may depend on the bacterial metabolic activity, division rate, etc. Conversely, μ may be imposed externally by, for example, pressure-based microfluidic flow-control systems in fluid chambers with periodic boundary conditions. We note that it is particularly instructive to consider the most common experimental setting corresponding to the case of closed boundary

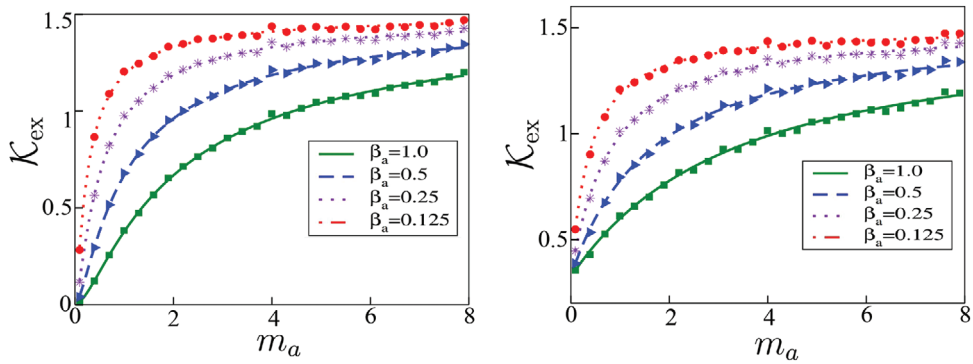

Figure 2. Excess kurtosis $\mathcal{K}_{ex}$ as a function of the mass m_a of the active particle for different values of β_a, for two different values of the active bath's mean kick amplitude: $\mu = 0$ (left panel), and $\mu = 2.0$ (right panel). Other simulation parameters were $\omega = 2.0$, $T = 0.5$, $\kappa = 2.0$, and $\gamma = 2.0$, total number of simulations 10^5, and simulation time step $dt = 10^{-4}$. In both panels, symbols are obtained from numerical simulations while lines are theoretical predictions given by Equation (64).

conditions,[15,36] $\lambda = 0$, for which we still get an enhancement of the variance with respect to the thermal reference value $k_B T/\kappa$.

As we have shown in Equation (55), the usage of equipartition theorem in recent experimental work in refs. [15, 36] is well-suited for the case $\mu = 0$

$$T_{\text{eff}} = \frac{\kappa \langle X^2 \rangle}{k_B} \tag{60}$$

For an equilibrium Langevin dynamics in the external potential $U(x) = \kappa x^2/2$, T_{eff} would be the temperature needed to attain the value $\langle X^2 \rangle$ of the second moment observed in the PSN active-bath model. For the PSN active noise with symmetric Gaussian kick amplitudes, we get via Equation (59) for $\lambda = 0$ that

$$T_{\text{eff}} = T + \left(\frac{\omega \tau_a}{2}\right) T_a \tag{61}$$

As expected, the PSN active noise leads to an effective temperature, that is always larger or equal than the bath temperature, that is, $T_{\text{eff}} \geq T$. Equation (61) implies that the effective temperature defined by Equation (60) is sensitive to two properties of the active bath, the rate of kicks ω, and the variance $\approx \tau_a T_a \propto T_a m_a$ of the kick amplitudes. For the case of colloidal heat engines in bacterial reservoirs the effective temperatures derived through Equation (60) were found to be up to one order of magnitude larger than the room temperature. For example in ref. [15] the bath temperature during the isothermal steps was $T \approx$ 300 K but the active temperature was found to be $T_{\text{eff}} \approx 1000$ K. Such enhancement of the effective temperature was linked to the efficiency enhancement in theoretical models of active heat engines[25–27,73,74] where exact non-Gaussian statistics and fluctuation response were not tackled.

We also compute the skewness of the distribution from Equation (39)

$$\tilde{\mu}_3[X] = \frac{\omega \tau \lambda}{3} \left(3 k_B T_a \frac{\tau_a}{\gamma} + \lambda^2\right) \left(\frac{k_B T}{\kappa} + \frac{\omega \tau}{2} \left(k_B T_a \frac{\tau_a}{\gamma} + \lambda^2\right)\right)^{-3/2} \tag{62}$$

This result shows that in the specific case of symmetric or extremely rare kicks, that is, small μ and ω, the skewness vanishes, as it should.

Let us conclude this subsection with the exact analytical expression for the excess kurtosis [see Equation (40)], which yields in the form

$$\mathcal{K}_{ex}[X] = \frac{3\omega\tau}{4} \left(\left(k_B T_a \frac{\tau_a}{\gamma}\right)^2 + \frac{\lambda^2}{3} \left(6 k_B T_a \frac{\tau_a}{\gamma} + \lambda^2\right)\right) \left(\frac{k_B T}{\kappa} + \frac{\omega\tau}{2} \left(k_B T_a \frac{\tau_a}{\gamma} + \lambda^2\right)\right)^{-2} \tag{63}$$

Equation (63) confirms that for any parameter value $\mathcal{K}_{ex}[X] \geq 0$ is always positive, indicating that the stationary distribution of the position is always leptokurtic in the case of Gaussian kicks. The detailed analysis of $\mathcal{K}_{ex}[X]$ is presented in Section 4.1 for various parameter regimes.

4.1. Results for $\mathcal{K}_{ex}$ and Deviation from the Gaussian Distribution to Non-Gaussianity and Re-Entry to Gaussianity

This section briefly discusses and concludes the analytical and numerical results of $\mathcal{K}_{ex}$ for the particular Gaussian form for the amplitude distribution $\rho_a(\gamma)$ given by Equation (56). The behavior of the Brownian particle in the presence of active PSN exhibits non-Gaussian dynamics. In the steady state, the excess kurtosis is quantified by Equation (63). In **Figure 2** we illustrate the relationship between $\mathcal{K}_{ex}$ and the mass m_a of the active particle across various values of β_a. Here, we examine two scenarios. In the left panel in Figure 2, we explore the behavior of the excess kurtosis in a setup where the particle is optically trapped within a closed container filled with bacteria. In this configuration, the active self-propelled bacteria exert net drift ($\mu = 0$) and move randomly inside the fluid container. The expression of the excess kurtosis in this case reads,

$$\mathcal{K}_{ex}[X] = \frac{3\omega\tau_a^2}{\tau} \left(\omega\tau_a + 2\frac{T}{T_a}\right)^{-2} \tag{64}$$

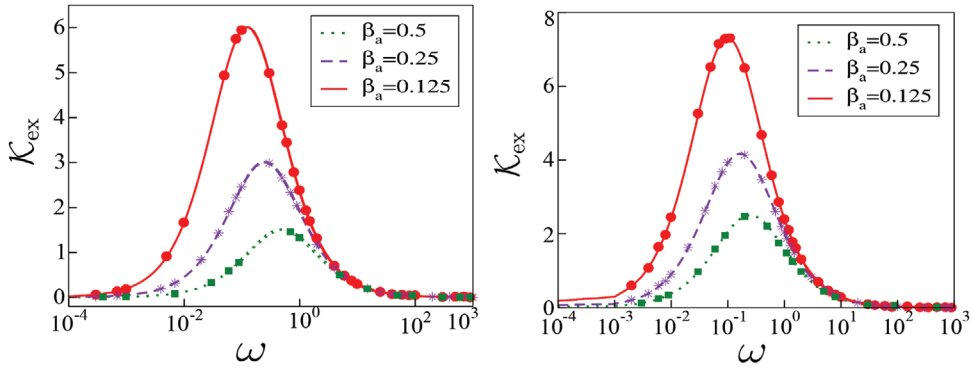

Figure 3. (Left panel) Excess kurtosis $\mathcal{K}_{ex}$ as a function of the kick rate ω for $\mu = 0.0$ for different values of β_a. (Right panel) Excess kurtosis $\mathcal{K}_{ex}$ as a function of the kick rate ω for $\mu = 2.0$. Here other Parameters used are $m_a = 2.0$, $T = 0.5$, $\kappa = 2.0$, $\gamma = 2.0$, number of simulations 10^5 and simulation time step $dt = 10^{-4}$. In both panels, symbols are obtained from numerical simulations while lines are theoretical predictions given by Equation (64).

We further compare these with the behavior of the kurtosis in the limits of m_a. It is evident that the mass of the bacteria plays a pivotal role in determining the system's dynamics. When m_a approaches zero, τ_a also tends to zero, resulting in the convergence to zero of the excess kurtosis $\mathcal{K}_{ex}$. Conversely, for large values of m_a and as τ_a approaches very large values, the excess kurtosis converges to $3/\omega\tau$.

In the right panel in Figure 2, we consider the scenario of an optically trapped particle within a bacterial bath under a uniform fluid flow, as illustrated in Figure 1. At large m_a (i.e., in the limit of $\tau_a \to \infty$) the value of the excess kurtosis increases and eventually saturates at the value $3/\omega\tau$ for fixed values of T_a and ω. Furthermore, when we increase the active temperature T_a for given m_a and ω, the non-Gaussianity of the system becomes more pronounced.

The preceding analysis thus reveals that the excess kurtosis reaches its asymptotic large m_a limit that is independent on the external torque μ. Furthermore, the active temperature T_a controls the sharpness of the transition between Gaussian ($\mathcal{K}_{ex} = 0$) to non-Gaussian ($\mathcal{K}_{ex} > 0$) behavior; the larger T_a the steeper is the transition from the minimum to the maximum value of the excess kurtosis as a function of m_a.

Next we analyze in **Figure 3** how the excess kurtosis $\mathcal{K}_{ex}$ depends on the kick rate ω. In the left panel in Figure 3 we observe that the degree of non-Gaussianity as measured by $\mathcal{K}_{ex}$ exhibits a non-monotonic dependency with ω. In the limit of ω small, the system has no active particles and behaves as a thermal system, resulting in a predominantly Gaussian behavior. As we increase ω, the number of kicks between the Brownian particle and the active particles becomes significant, effecting a substantial enhancement of the system dynamics, pushing it out of equilibrium and increasing the non-Gaussian behavior. Interestingly, however, in the limit of ω large, the Brownian particle is kicked by the active particles even more frequently and in a more random fashion. Consequently, the system tends toward Gaussian white noise with finite intensity, restoring Gaussianity. This process illustrates the transition from Gaussian to non-Gaussian behavior and the subsequent return to Gaussianity, known as re-entry into the Gaussian regime. This signifies the crossover from passive to active and back to (effectively) passive behavior.

Furthermore, by keeping T, κ, and the distribution $\rho_a(\gamma)$ fixed, it is possible to identify an optimal value of ω that maximizes the excess kurtosis. This optimal value for ω reads

$$\omega^* = \frac{2k_B T\beta_a}{\tau_a + \lambda^2\beta_a\gamma} \tag{65}$$

corresponding to the maximum value of $\mathcal{K}_{ex}[X]$

$$\mathcal{K}^*_{ex}[X] = \left(\frac{\frac{3\tau_a^2}{\beta_a} + 6\tau_a\lambda^2\beta_a\gamma + \beta_a\gamma^2\lambda^4}{8\tau k_B T\left(\tau_a + \beta_a\gamma\lambda^2\right)} \right) \tag{66}$$

In **Figure 4**, the left panel illustrates the relationship between the excess kurtosis $\mathcal{K}_{ex}$ and the rate ω of kicks for a specific value of T_a. Here Equation (66) is used to identify the maximum value $\mathcal{K}^*_{ex}$ and the corresponding optimal rate ω^*. In the right panel, we use the value of ω^* to examine the displacement PDF of the Brownian particle and compare it with the Gaussian PDF. The plot distinctly illustrates that the active distribution exhibits tails that are significantly wider than in comparison to the shorter tails of the Gaussian distribution associated with the equilibrium state $\omega = 0$.

5. Conclusion and Discussion

We presented a combined analytical and numerical approach to compute higher order moments and the PDF for a colloidal particle in a thermal bath which experiences additional Poisson-shot noise in an active environment for the case of a harmonic trapping. Our formulation includes a general amplitude PDF of the kicks due to the active particles. The latter are considered for both cases with and without a net drift. In the non-equilibrium steady state we quantify the skewness and non-Gaussianity of the emerging PDF and discuss the effective temperature of the system. Concretely for a Gaussian amplitude PDF of the shot noise we obtain exact results for the excess kurtosis and demonstrate that the stationary PDF is leptokurtic, with a narrow central region and heavy tails.

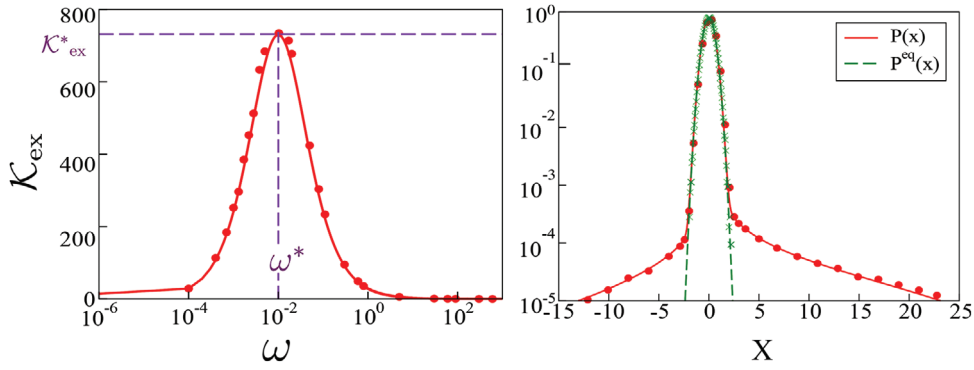

Figure 4. (Left panel) Excess kurtosis $\mathcal{K}_{ex}$ as a function of the kick rate ω obtained from numerical simulations (red circles) and compared with the theoretical prediction (red solid line, Equation (64)). The vertical dashed purple line is set at the optimal value of the kick rate ω^* [Equation (65)] maximizing the excess kurtosis at a value $\mathcal{K}^\star_{ex}$ [Equation (66)]. (Right panel) Probability density for the position of the Brownian particle obtained from numerical obtained from numerical simulations (red circles). The lines are given by the analytical solution of the stationary density ($P(x)$, red solid line) and the (Gaussian) equilibrium distribution in the absence of kicks ($P^{eq}(x)$, green dashed line). Other simulation parameters were $m_a = 2.0$, $T = 0.5$, $\kappa = 2.0$, $\gamma = 0.2$, $\mu = 0.0$, number of simulations 10^5, and simulation time step $dt = 10^{-4}$.

Our model and analysis provides a flexible platform to describe 1D experimental systems that are characterized by nonequilibrium stationary states with fat tails. A key advantage with respect to other solvable models, such as the AOUP, is the fact that the stationary state of our model is in general non-Gaussian. Moreover, unlike many ad-hoc active-matter accounts, our model reconciles the fluctuation-dissipation theorem and the equipartition theorem for any active kick distribution with zero mean. This makes our description of singular interest to experimentalists who will likely benefit from our inference method developed in Section 3.2. We expect our approach to impact ongoing research on stochastic thermodynamics of active systems, for which we outline some preliminary ideas below.

The analytical approach developed here may find applications in the stochastic thermodynamics of active matter. We here add some remarks on some open questions regarding irreversibility and dissipation associated with the dynamics of the non-equilibrium stationary state induced by the active PSN. As noted, since the foundations of stochastic thermodynamics, quantifying the asymmetry under time reversal of a stationary time series, provides means to estimate the underlying entropy production of the physical mechanism generating the time series.[80] Within this context, it was shown that the rate of irreversibility measured by the Kullback-Leibler (KL) divergence rate

$$\sigma = \lim_{t\to\infty} \frac{1}{t} \int \mathcal{D}x_{[0,t]} P(x_{[0,t]}) \ln \frac{P(x_{[0,t]})}{P(\Theta_t x_{[0,t]})} \geq 0, \tag{67}$$

provides a lower bound to the steady-state rate of entropy production. Equation (67) can be understood as the KL divergence rate between the probability of trajectories and their time reversal. In other words, $P(x_{[0,t]}) = P(X_0 = x_0, \dots X_t = x_t)$ is the probability to observe the sequence $x_0, \dots, x_t$ in the time interval $[0, t]$, and $P(\Theta_t x_{[0,t]}) = P(X_0 = x_t, \dots X_t = x_0)$ the probability to observe the time-reversed sequence $x_t, \dots, x_0$ in the same time interval $[0, t]$, where both P and $P(\Theta_t)$ are evaluated at the stationary state. Our active-matter model given by Equation (1) displays time irreversibility in the presence of PSN. Indeed by inspection of the time series shown in the right panel of Figure 1) one finds that rapid changes in the particle position due to active kicks are often accompanied by slow relaxations—a dynamics being time irreversible even for the case of symmetric PSN with vanishing net velocity $\mu = 0$. Thus, in general one has $\sigma > 0$ as a signature of irreversibility whenever $\omega > 0$. Conversely, since the dynamics is bounded by the confining potential, one can show that the particle energy $U_t = (1/2)\kappa X_t^2$, which fluctuates over time, is conserved on average, leading to a vanishing heat dissipation rate. This leads us to conclude that traditional probes of irreversibility such as heat dissipation are not sufficient to characterize the non-equilibrium features of the PSN; instead, one should take an information-theoretical approach, for example, by evaluating σ in Equation (67), or using cross-correlation asymmetries as discussed below.

Evaluating the irreversibility rate (67) for our model is not an easy task, both analytically and from numerical estimates. We here discuss some alternatives to quantify the degree of time irreversibility. First we note that because the dynamics is 1D and with open boundary conditions, the stationary probability current vanishes. This implies that $P(x_{t_1}, x_{t_2}) = P(x_{t_2}, x_{t_1})$; in other words, one cannot detect irreversibility from the autocorrelation function of the position. In general, however, $P(x_{t_1}, x_{t_2}, x_{t_3}) \neq P(x_{t_3}, x_{t_2}, x_{t_1})$ even in the absence of a net current in X,[80] which reveals that the $(n \geq 3)$th time correlators of the particle position $\langle X_{t_1} \dots X_{t_n} \rangle$ could be used to characterize the irreversibility of our model. Following Steinberg,[81] an alternative approach is to consider two-time correlators including non-linear functions of the observables. For example, let us consider the following two-time cross-correlators of the position and of its third power,

$$C^{X,X^3}_{t_1,t_2} \equiv \langle X_{t_1} (X_{t_2})^3 \rangle, \quad C^{X^3,X}_{t_1,t_2} \equiv \langle (X_{t_1})^3 X_{t_2} \rangle. \tag{68}$$

Figure 5 shows numerical estimates of the correlators $C^{X,X^3}_{t_1,t_2}$ (red solid line) and $C^{X^3,X}_{t_1,t_2}$ (green dashed line) for the case of symmetric Gaussian kicks ($\mu = 0$) with zero kick rate $\omega = 0$ (left panel) and non-zero kick rate $\omega > 0$ (right panel). Our analysis reveals an asymmetry between the X, X^3 cross-correlators $C^{X,X^3}_{t_1,t_2} \neq C^{X^3,X}_{t_1,t_2}$ in the presence of active kicks for all values of t_1 and t_2 that we

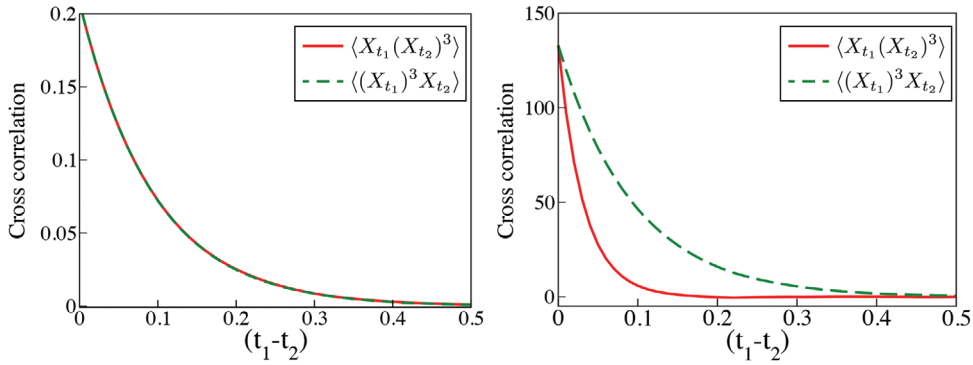

Figure 5. Cross-correlation asymmetry in the presence of active Poissonian shot noise (PSN) with amplitudes drawn from the Gaussian distribution (56). Left panel: Comparison between the forward and backward X, X^3 cross-correlation functions (68) for an equilibrium dynamics given by Equation (1) without active PSN (i.e., vanishing rate of kicks $\omega = 0$). Right panel: Comparison between the forward and backward X, X^3 cross-correlation functions (68) in the presence of PSN with rate of kicks $\omega = 10^{-2}$. Other simulation parameters are $T = 0.5$, $\kappa = 2.0$, $\gamma = 0.2$, $m_a = 2.0$, $\mu = 0.0$, and $T_a = 8.0$, number of simulations 10^5, and simulation time step $dt = 10^{-4}$.

explored, and vice versa a symmetry $C^{X,X^3}_{t_1,t_2} = C^{X^3,X}_{t_1,t_2}$ for all t_1, t_2 in the absence of active noise. Our numerical result reinforces recent insights from stochastic thermodynamics which have unveiled the difference of cross-correlators, for example, $|C^{X,X^3}_{t_1,t_2} - C^{X^3,X}_{t_1,t_2}|$, as probes of the degree of non-equilibrium.[82–86] Such results have provided lower bounds to the rate of irreversibility σ of Markovian systems that are directly proportional to the asymmetry of cross correlators. It will be interesting in the future to relate our findings to these novel approaches to tackle irreversibility and dissipation through non-trivial cross-correlation structures.

We finally remark that while the harmonic oscillator is the most fundamental model in statistical physics, cases of anharmonic external potentials should also be considered in the presence of fluctuating forces different from white Gaussian noise. Thus, processes with Gaussian yet long-range dependent noises exhibit non-Boltzmannian stationary PDFs in the presence of steeper than harmonic potentials or do not possess a stationary state in shallower than harmonic potentials.[87–89] It will thus be interesting to see how particles driven by both thermal noise and PSN perform in anharmonic potentials.

Appendix

Appendix A: Moments of X_2

We here prove Equations (33)–(35) introduced in the main text. They can all be straightforwardly proven using identities (22) and (32). Since those two identities involve derivatives of $I(q)$ evaluated at $k = 0$, it will be convenient to find first a general expression for $\frac{d^n}{dq^n} I(q)|_{q=0}$.

A.1. Derivatives of $I(q)$

Derivatives of $I(q)$ can be easily obtained by means of the Taylor series. First, from the definition of $I(q)$, Equation (19), it is clear that $I(0) = 0$. Equation (19) can also be used to find all derivatives of $I(q)$ denoted by $I^{(n)}(0)$. Let us start from the Taylor expansion of $\hat{\rho}_a(q)$ around $k = 0$

$$\hat{\rho}_a(q) = \sum_{n=0}^{\infty} \frac{1}{n!} \hat{\rho}_a^{(n)}(0) q^n \tag{A1}$$

where $\hat{\rho}_a^{(n)}$ denotes the nth derivative of $\hat{\rho}_a$. The last expression substituted into Equation (19) gives the first derivative of $I(q)$,

$$I'(q) = \frac{\hat{\rho}_a(q) - \hat{\rho}_a(0)}{q} = \sum_{n=1}^{\infty} \frac{1}{n!} \hat{\rho}_a^{(n)}(0) q^{n-1} \tag{A2}$$

Taking $m - 1$ derivatives in k we obtain

$$\frac{d^m}{dq^m} I(q) = \sum_{n=m}^{\infty} \frac{(n-1)(n-2)\ldots(n-m+1)}{n!} \hat{\rho}_a^{(n)}(0) q^{n-m} \tag{A3}$$

which, evaluated at $q = 0$, yields

$$I^{(m)}(0) = \frac{1}{m} \hat{\rho}_a^{(m)}(0) \text{ for } m \geq 1 \tag{A4}$$

The moments of ρ_a are related to the derivatives of $\hat{\rho}_a$ through the relation $\langle Y^m \rangle_a = \frac{1}{i^m} \hat{\rho}^{(m)}(0)$. Hence

$$I^{(m)}(0) = \frac{i^m}{m} \langle Y^m \rangle_a \tag{A5}$$

We will make use of this result in the next subsection.

A.2. Moments of X_2

We nowprove Equations (33)–(35). For the first we immediately see that

$$\langle X_2 \rangle = \frac{1}{i} \frac{d}{dk} \hat{P}_2(q)\Big|_{q=0} = \frac{1}{i} \omega\tau I'(0) = \omega\tau \langle Y \rangle_a \tag{A6}$$

where we use expression (17) for $\hat{P}_2(q)$ and Equation (A5). To prove Equations (34) and (35) for simplicity we define $f(q) \equiv I(q) - qI'(0)$; according to Equation (32) we need to take the derivatives of $\exp(\omega\tau f(q))$. The second derivative evaluated at $q = 0$ reads

$$\begin{aligned} \frac{d^2}{dq^2} \exp(\omega\tau f(q))|_{q=0} &= \left[\left(\omega^2\tau^2 f'(q)^2 + \omega\tau f''(q) \right) \exp(\omega\tau f(q)) \right]|_{q=0} \\ &= \omega\tau I^{(2)}(0) \end{aligned} \tag{A7}$$

since $f(0) = f'(0) = 0$ and $f^{(n)}(0) = I^{(n)}(0)$. Using this expression along with Equations (32) and (A5) we obtain for the second moment

$$\langle (X_2 - \langle X_2 \rangle)^2 \rangle = \frac{1}{2}\omega\tau\langle Y^2 \rangle_a \tag{A8}$$

which proves Equation (34), where $n = 2$. Analogously, now consider the third derivative of $\exp(\omega\tau f(q))$

$$\frac{d^3}{dq^3}\exp(\omega\tau f(q))|_{q=0} = \left[\left(\omega^3\tau^3 f'(q)^3 + 3\omega^2\tau^2 f'(q)f''(q) + \omega\tau f'''(q)\right)\exp(\omega\tau f(q))\right]|_{q=0} = \omega\tau I^{(3)}(0) \tag{A9}$$

Thus the third central moment of X_2 reads

$$\langle (X_2 - \langle X_2 \rangle)^3 \rangle = \frac{1}{3}\omega\tau\langle Y^3 \rangle_a \tag{A10}$$

proving Equation (34), where $n = 3$. To prove Equation (35) we consider the fourth derivative

$$\frac{d^4}{dq^4}\exp(\omega\tau f(q))|_{q=0} = \Big[\left(\omega^4\tau^4 f'(q)^4 + 6\omega^3\tau^3 f'(q)^2 f''(q) + 3\omega^2\tau^2 f''(q)^2 + 4\omega\tau^2 f^{(3)}(q)f'(q) + \omega\tau f^{(4)}(q)\right)\exp(\omega\tau f(q))\Big]\Big|_{q=0}$$
$$= 3\omega^2\tau^2\left(I^{(2)}(0)\right)^2 + \omega\tau I^{(4)}(0) \tag{A11}$$

Hence, we have

$$\langle (X_2 - \langle X_2 \rangle)^4 \rangle = \frac{3}{4}\omega^2\tau^2\langle Y^2 \rangle_a^2 + \frac{1}{4}\omega\tau\langle Y^4 \rangle_a \tag{A12}$$

Which completes our proof.

Appendix B: Time-Dependent Moments

In most of our work, we have just considered the moments of the stationary distribution. Since the time-dependent distribution is not available, we do not have access to the time evolution of the moments of the position. Nevertheless, starting from the Fokker–Planck equation, we can construct a set of ordinary differential equations for the finite-time moments $\langle X_t^n \rangle$ for $n \in \mathbb{N}$. By multiplying Equation (11) by x^n and integrating over x we obtain

$$\tau\frac{\partial}{\partial t}\langle X_t^n \rangle = -n\langle X_t^n \rangle + \frac{k_B T}{\kappa}n(n-1)\langle X_t^{n-2} \rangle + \omega\tau\left(\langle (X_t + Y)^n \rangle - \langle X_t^n \rangle\right) \tag{B1}$$

with the convention that $\langle X_t^{-1} \rangle = 0$, and

$$\langle (X_t + Y)^n \rangle = \int_{-\infty}^{\infty}\int_{-\infty}^{\infty}(x+y)^n P(x,t)\rho_a(y)\,dxdy \tag{B2}$$

Equation (B1) can be rewritten using the binomial formula

$$\tau\frac{\partial}{\partial t}\langle X_t^n \rangle = -n\langle X_t^n \rangle + \frac{k_B T}{\kappa}n(n-1)\langle X_t^{n-2} \rangle + \omega\tau\sum_{m=0}^{n-1}\binom{n}{m}\langle X_t^m \rangle\langle Y^{n-m} \rangle_a \tag{B3}$$

Therefore, we find a hierarchy of relations for the generic nth moment in terms of the first to the $(n-1)$th moment. A general analytical solution to Equation (B3) is not straightforward, nevertheless equations governing the first two moments are relatively simple

$$\tau\frac{\partial}{\partial t}\langle X_t \rangle = -\langle X_t \rangle + \omega\tau\langle Y \rangle_a \tag{B4}$$

$$\tau\frac{\partial}{\partial t}\langle X_t^2 \rangle = -2\langle X_t^2 \rangle + 2\frac{k_B T}{\kappa} + \omega\tau\langle Y^2 \rangle_a + 2\omega\tau\langle X_t \rangle\langle Y \rangle_a \tag{B5}$$

thus the first moment reads

$$\langle X_t \rangle = \langle X_0 \rangle\exp(-t/\tau) + (1 - \exp(-t/\tau))\omega\tau\langle Y \rangle_a \tag{B6}$$

while the second moment

$$\langle X_t^2 \rangle = \langle X_0^2 \rangle e^{-2t/\tau} + \left(\frac{k_B T}{\kappa} + \frac{\omega\tau}{2}\langle Y^2 \rangle_a\right)[1 - \exp(-t/\tau)] \tag{B7}$$
$$+ 2\omega\tau\langle Y \rangle_a\langle X_0 \rangle[\exp(-t/\tau) - \exp(-2t/\tau)]$$
$$+ \omega^2\tau^2\langle Y \rangle_a^2[\exp(-2t/\tau) - 2\exp(-t/\tau) + 1] \tag{B8}$$

It is then possible to obtain the variance which reads

$$\mathrm{Var}[X_t] = \left(\frac{k_B T}{\kappa} + \frac{\omega\tau}{2}\langle Y^2 \rangle_a\right)[1 - \exp(-t/\tau)] \tag{B9}$$

Despite the presence of the Poissonian shot noise, the system relaxes to its stationary state with a characteristic time τ that does not depend on the rate of the kicks.

Appendix C: Derivation of Susceptibility

We will here expose the analytical derivation of the function $\chi_X(t)$ (50). The average of $\langle X_t \rangle_{\delta f}$ can be obtained with a minimal modification of Equation (B1)

$$\tau\frac{\partial}{\partial t}\langle X_t \rangle_{\delta f} = -\langle X_t \rangle_{\delta f} + \frac{\delta f}{\kappa} + \omega\tau\langle Y \rangle_a \tag{C1}$$

Clearly, since the perturbation is independent from the noise η_t, the moments of Y remain unaltered. The susceptibility will then read

$$\chi_X(t) = \frac{1}{\kappa}(1 - \exp(-t/\tau)) \tag{C2}$$

which at stationarity becomes

$$\chi_X = \frac{1}{\kappa} \tag{C3}$$

Appendix D: Numerical Simulations

We conclude the paper with a short discussion on how to simulate the system. Trajectories evolving with the Langevin equation can be generated via the Euler–Maruyama scheme described in any textbook on numerical implementation of stochastic differential equations (we refer to ref. [90]). While the analytical expression (18) can be simulated using the GNU Scientific Library (GSL) available in many languages (we used the Julia language[79]). To calculate Equation (18) we proceeded in three steps: (i) we compute the function $I(q)$ in Equation (19) for a discrete set of values of q; (ii) we interpolate the resulting values with a cubic spline interpolation available in the package `Interpolations.jl` in order to find a continuous version of $I(q)$; (iii) we plug this function into formula (18) and integrate for a range of values of x. All numerical integrations were performed using the Gauss–Kronrod algorithm available in the package `QuadGK.jl`. We simulate the Langevin system 1 using the first-order integrator method. The Gaussian noise ξ_t is derived from the Wiener process, and the active kicks are generated at Poisson-distributed times with rate ω.

Acknowledgements

C.D.B and R.M. contributed equally to this work. The authors thank Kiyoshi Kanazawa and Dario Lucente for useful discussions. Rah.M. gratefully acknowledges Science and Engineering Research Board (SERB), India for financial support through the MATRICS Grant (No. MTR/2020/000349). Ri.M. acknowledges Sandwich Training Educational Programme (STEP) by Abdus Salam International Center for Theoretical Physics (ICTP), Trieste, Italy. Ra.M. acknowledges the German Science Foundation (DFG, grant ME 1535/12-1) for financial support. É.R. acknowledges financial support from PNRR MUR project PE0000023-NQSTI.

Conflict of Interest

The authors declare no conflict of interest.

Data Availability Statement

The data that support the findings of this study are available from the corresponding author upon reasonable request.

Keywords

active matter, Brownian motion, non-Gaussian fluctuations, stochastic processes

Received: September 22, 2023
Revised: December 5, 2023
Published online:

[1] A. Einstein, *Ann. Phys.* **1905**, *322*, 549.
[2] M. von Smoluchowski, *Ann. Phys.* **1906**, *21*, 756.
[3] P. Langevin, *C. R. Acad. Sci.* **1908**, *146*, 530.
[4] P. Lévy, Processus Stochastiques et Mouvement Brownien, Gauthier-Villars, Paris **1948**.
[5] R. Zwanzig, *Nonequilibrium Statistical Mechanics*, Oxford University Press, Oxford**2001**.
[6] W. Brenig, *Statistical Theory of Heat: Nonequilibrium Phenomena*, Springer, Berlin, Heidelberg**1989**.
[7] R. Kubo, M. Toda, N. Hashitsume, *Statistical Physics II: Nonequilibrium Atatistical Mechanics*, Springer, Berlin, Heidelberg**1985**.
[8] N. G. van Kampen, *Stochastic Processes in Physics and Chemistry*, North-Holland, Amsterdam, **1981**.
[9] L. D. Landau, E. M. Lifshitz, *Landau and Lifshitz Course of Theoretical Physics 5: Statistical Physics Part 1*, Butterworth-Heinemann, Oxford, **1980**.
[10] K. Sekimoto, *Prog. Theor. Phys.* **1998**, *130*, 17.
[11] U. Seifert, *Rep. Prog. Phys.* **2012**, *75*, 126001.
[12] T. Vicsek, A. Zafeiris, *Phys. Rep.* **2012**, *517*, 71.
[13] S. Ramaswamy, *Ann. Rev. Cond. Mat. Phys.* **2010**, *1*, 323.
[14] C. Bechinger, R. D. Leonardo, H. Löwen, C. Reichhardt, G. Volpe, G. Volpe, *Rev. Mod. Phys.* **2016**, *88*, 045006.
[15] S. Krishnamurthy, S. Ghosh, D. Chatterji, R. Ganapathy, A. K. Sood, *Nat. Phys.* **2016**, *12*, 1134.
[16] D. Loi, S. Mossa, L. F. Cugliandolo, *Phys. Rev. E* **2008**, *77*, 051111.
[17] C. Maes, *J. Stat. Phys.* **2014**, *154*, 705.
[18] C. Maes, S. Steffenoni, *Phys. Rev. E* **2015**, *91*, 022128.
[19] E. Fodor, C. Nardini, M. E. Cates, J. Tailleur, P. Visco, F. van Wijland, *Phys. Rev. Lett.* **2016**, *117*, 038103.
[20] F. S. Gnesotto, F. Mura, J. Gladrow, C. P. Broedersz, *Rep. Prog. Phys.* **2018**, *81*, 066601.
[21] É. Roldán, J. Barral, P. Martin, J. M. R. Parrondo, F. Jülicher, *New J. Phys.* **2021**, *23*, 083013.
[22] J. Spiechowicz, J Łuczka, P. Hänggi, *J. Stat. Mech.* **2013**, *2013*, P02044.
[23] U. Basu, S. N. Majumdar, A. Rosso, S. Sabhapandit, G. Schehr, *J. Phys. A* **2020**, *53*, 09LT01.
[24] A. Saha, R. Marathe, A. M. Jayannavar, *J. Stat. Mech.* **2018**, *2018*, 113203.
[25] A. Saha, R. Marathe, *J. Stat. Mech.* **2019**, *2019*, 094012.
[26] R. Majumdar, A. Saha, R. Marathe, *J. Stat. Mech.* **2022**, *2022*, 073206.
[27] C. A. Guevara-Valadez, R. Marathe, J. R. Gómez-Solano, *Phys. A* **2023**, *609*, 128342.
[28] D. Chaudhuri, A. Dhar, *J. Stat. Mech.* **2021**, *2021*, 013207.
[29] D. Lucente, A. Puglisi, M. Viale, A. Vulpiani, *Phys. Rev. Lett.* **2023**, *131*, 078201.
[30] A. Shee, D. Chaudhuri, *Phys. Rev. E* **2022**, *105*, 054148.
[31] K. Nørregaard, R. Metzler, C. Ritter, K. Berg-Sørensen, L. Oddershede, *Chem. Rev.* **2017**, *117*, 4342.
[32] J-.H. Jeon, N. Leijnse, L. Oddershede, R. Metzler, *New J. Phys.* **2013**, *15*, 045011.
[33] V. Blickle, C. Bechinger, *Nat. Phys.* **2012**, *8*, 143.
[34] I. A. Martínez, É. Roldán, L. Dinis, D. Petrov, J. M. R. Parrondo, R. A. Rica, *Nat. Phys.* **2016**, *12*, 67.
[35] X. L. Wu, A. Libchaber, *Phys. Rev. Lett.* **2000**, *84*, 3017.
[36] N. Roy, N. Leroux, A. K. Sood, R. Ganapathy, *Nat. Commun.* **2021**, *12*, 4927.
[37] J. A. C. Albay, Z.-Y. Zhou, C.-H. Chang, Y. Jun, *Sci. Rep.* **2021**, *11*, 4394.
[38] K. Cheng, P. Liu, M. Yang, M. Hou, *Soft Matter* **2022**, *18*, 2541.
[39] We note that non-Gaussian tails have also been shown for the unconfined active motion of polymers in active particle baths,[40] microswimmers,[41] social amoeba,[43] self-propelling Janus particles,[42] progenitor cells,[44] or nematodes,[45] for which distributed-parameter models have been discussed.[46, 47]
[40] J. Shin, A. G. Cherstvy, W. K. Kim, R. Metzler, *New J. Phys.* **2015**, *17*, 113008.
[41] K. C. Leptos, J. S. Guasto, J. P. Gollub, A. I. Pesci, R. E. Goldstein, *Phys. Rev. Lett.* **2009**, *103*, 198103.
[42] X. Zheng, B. Hagen, A. Kaiser, M. Wu, H. Cui, Z. Silber-Li, H. Löwen, *Phys. Rev. E* **2013**, *88*, 032304.
[43] A. Cherstvy, O. Nagel, C. Beta, R. Metzler, *Phys. Chem. Chem. Phys.* **2018**, *20*, 23034.
[44] B. Partridge, S. Gonzalez Anton, R. Khorshed, G. Adams, C. Pospori, C. L. Celso, C. F. Lee, *PLoS ONE* **2022**, *17*, e0272587.
[45] S. Hapca, J. Crawford, I. Young, *J. R. Soc. Interface* **2008**, *6*, 111.
[46] S. M. J. Khadem, N. H. Siboni, S. H. L. Klapp, *Phys. Rev. E* **2021**, *104*, 064615.
[47] E. Lemaitre, I. M. Sokolov, R. Metzler, A. V. Chechkin, *New J. Phys.* **2023**, *25*, 013010.
[48] R. F. Fox, *Phys. Rev. A* **1986**, *33*, 467.
[49] P. Jung, P. Hänggi, *Phys. Rev. A* **1987**, *35*, 4464.
[50] J. Tailleur, M. E. Cates, *EPL* **2009**, *86*, 60002.
[51] C. Maggi, U. M. B. Marconi, N. Gnan, R. Di Leonardo, *Sci. Rep.* **2015**, *5*, 10742.
[52] A. Gopal, É. Roldán, S. Ruffo, *J. Phys. A* **2021**, *54*, 164001.
[53] É. Fodor, C. Nardini, M. E. Cates, J. Tailleur, P. Visco, F. van Wijland, *Phys. Rev. Lett.* **2016**, *117*, 038103.
[54] J. T. Park, G. Paneru, C. Kwon, S. Granick, H. K. Pak, *Soft Matter* **2020**, *16*, 8122.
[55] P. Hänggi, *Z. Phys. B* **1978**, *30*, 85.
[56] P. Hänggi, *Z. Phys. B* **1980**, *36*, 271.
[57] I. Eliazar, J. Klafter, *J. Stat. Phys.* **2003**, *111*, 739.
[58] C. van den Broeck, *J. Stat. Phys.* **1983**, *31*, 467.
[59] J. Spiechowicz, P. Hänggi, J. Łuczka, *Phys. Rev. E* **2014**, *90*, 032104.

[60] J. Spiechowicz, J. Łuczka, *Phys. Scr.* **2015**, *2015*, 014015.
[61] K. Białas, J. Łuczka, J. Spiechowicz, *Phys. Rev. E* **2023**, *107*, 024107.
[62] K. Kanazawa, T. G. Sano, T. Sagawa, H. Hayakawa, *Phys. Rev. Lett.* **2015**, *114*, 090601.
[63] K. Kanazawa, T. G. Sano, T. Sagawa, H. Hayakawa, *J. Stat. Phys.* **2015**, *160*, 1294.
[64] K. Białas, J. Łuczka, P. Hänggi, J. Spiechowicz, *Phys. Rev. E* **2020**, *102*, 042121.
[65] A. Baule, P. Sollich, *Sci. Rep.* **2023**, *13*, 3853.
[66] A. V. Chechkin, F. Seno, R. Metzler, I. M. Sokolov, *Phys. Rev. X* **2017**, *7*, 021002.
[67] C. Kim, E. Kyun Lee, P. Hänggi, P. Talkner, *Phys. Rev. E* **2007**, *76*, 011109.
[68] M. Grigoriu, *Phys. Rev. E* **2009**, *80*, 026704.
[69] M. B. Miller, *Mathematics and Statistics for Financial Risk Management*, 2nd ed., Wiley, New York, **2013**.
[70] P. Hänggi, *Z. Phys. B* **1989**, *75*, 275.
[71] A. Barato, U. Seifert, *Phys. Rev. Lett.* **2015**, *115*, 188103.
[72] T. Wampler, A. Barato, *J. Phys. A* **2021**, *55*, 014002.
[73] V. Holubec, S. Steffenoni, G. Falasco, K. Kroy, *Phys. Rev. Res.* **2020**, *2*, 043262.
[74] V. Holubec, R. Marathe, *Phys. Rev. E* **2020**, *102*, 060101.
[75] R. Zakine, A. Solon, T. Gingrich, F. van Wijland, *Entropy* **2017**, *19*, 193.
[76] L. Onsanger, *Phys. Rev.* **1930**, *37*, 405.
[77] L. Onsanger, *Phys. Rev.* **1931**, *38*, 2265.
[78] A. Crisanti, F. Ritort, *J. Phys. A: Math. Gen.* **2003**, *36*, R181.
[79] J. Bezanson, A. Edelman, S. Karpinski, V. B. Shah, *SIAM Rev.* **2017**, *59*, 1.
[80] É. Roldán, J. M. R. Parrondo, *Phys. Rev. Lett.* **2010**, *105*, 150607.
[81] I. Z. Steinberg, *Biophys. J.* **1986**, *50*, 171.
[82] N. Ohga, S. Ito, A. Kolchinsky, *Phys. Rev. E* **2023**, *131*, 077101.
[83] N. Shiraishi, arXiv:2304.12775 **2023**.
[84] T. V. Vu, V. T. Vo, K. Saito, arXiv:2305.18000 **2023**.
[85] S. Liang, S. Pigolotti, arXiv:2308.14497 **2023**.
[86] L. Oberreiter, U. Seifert, A. C. Barato, *Phys. Rev. E* **2022**, *106*, 014106.
[87] T. Guggenberger, A. Chechkin, R. Metzler, *J. Phys. A* **2021**, *54*, 29LT01.
[88] T. Guggenberger, A. V. Chechkin, R. Metzler, *New J. Phys.* **2022**, *24*, 073006.
[89] T. Vojta, S. Halladay, S. Skinner, S. Janušonis, T. Guggenberger, R. Metzler, *Phys. Rev. E* **2020**, *102*, 032108.
[90] P. E. Kloeden, E. Platen, *Numerical Solution of Stochastic Differential Equations*, Springer, Berlin, Heidelberg**2013**.